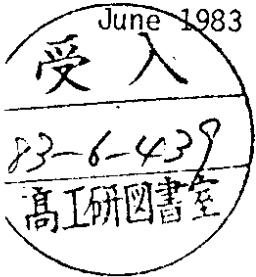


DESY 83-039  
June 1983



RECENT RESULTS FROM JADE ON ELECTROWEAK INTERACTIONS

by

Beate Naroska

ISSN 0418-9833

NOTKESTRASSE 85 · 2 HAMBURG 52

DESY behält sich alle Rechte für den Fall der Schutzrechtserteilung und für die wirtschaftliche Verwertung der in diesem Bericht enthaltenen Informationen vor.

DESY reserves all rights for commercial use of information included in this report, especially in case of filing application for or grant of patents.

To be sure that your preprints are promptly included in the  
HIGH ENERGY PHYSICS INDEX ,  
send them to the following address ( if possible by air mail ) :

DESY  
Bibliothek  
Notkestrasse 85  
2 Hamburg 52  
Germany

RECENT RESULTS FROM JADE ON ELECTROWEAK INTERACTIONS\*

Beate Naroska  
DESY  
Notkestr. 85  
D-2000 Hamburg 52

1) INTRODUCTION

The Jade collaboration<sup>1</sup> has performed measurements at Petra at an average center-of-mass (cms) energy of  $W \sim 35$  GeV in order to test Quantum Electrodynamics (QED) and electroweak theories. QED tests are still possible because the influence of the neutral weak current is negligible in many places, e.g. in  $e^+e^- \rightarrow \gamma\gamma$ , or in the total cross sections for  $e^+e^- \rightarrow e^+e^-$ ,  $\gamma\gamma$ ,  $\mu^+\mu^-$ , and  $\tau^+\tau^-$ . On the other hand the interference of the electromagnetic and the weak amplitudes leads to an asymmetry in the angular distributions of  $\mu^+\mu^-$  and  $\tau^+\tau^-$ , which was established for the first time at Petra. The measurements can be compared to predictions of electroweak theories, in particular the "standard model" of Glashow, Salam, and Weinberg<sup>2</sup>, which has successfully described neutral current phenomena in neutrino scattering<sup>3</sup> and polarized e-d scattering<sup>4</sup>. The tests at Petra were performed at a  $Q^2$  much higher than previously available.

In these reactions the contributions from diagrams of higher orders in  $\alpha$ , the QED coupling constant, lead to significant corrections, and it becomes important to check these corrections experimentally. Jade has performed measurements of the process  $e^+e^- \rightarrow \gamma\gamma$ , and  $\mu^+\mu^- \gamma$ , which provide an important check of radiative corrections, i.e. available calculations to order  $\alpha^3$ .

In the total cross section for  $e^+e^- \rightarrow$  hadrons, QCD corrections play an important role in addition to the electroweak effects. A careful study of the systematic errors of R was undertaken in order to derive results on the running coupling constant  $\alpha_s$  and the weak mixing angle  $\sin^2\theta_W$ .

\*Talk presented at the Europhysics Conference on Electroweak Effects at High Energies, Erice, February 1983. In this report only Jade results will be discussed. A comparison of experiments can be found in A. Boehm's talk in the proceedings of the same conference.

Finally a search for new heavy leptons, which occur in some models, is reported. Limits for the mass of excited states of the electron and muon, for a new sequential heavy lepton, and for a neutral heavy lepton are given.

The Jade detector was described in ref. 5. Its central tracking device is the "jet chamber". Rodoscopes of leadglass are used as electromagnetic shower detector and muons are detected in a segmented muon filter.

2) THE ELECTROWEAK CROSS SECTION

In lowest order the differential cross section for  $e^+e^- \rightarrow f^+f^-$ , where f can be a  $\mu$ ,  $\tau$ , or quark, assuming factorisation, is<sup>6</sup>:

$$(1) \quad d\sigma/d\Omega = \frac{\alpha^2}{4s} \cdot (C_1 \cdot (1 + \cos^2\theta) + C_2 \cdot \cos\theta)$$

$$\text{with } C_1 = Q_f^2 - 2 \cdot Q_f \cdot v_e v_f \chi + (v_e^2 + a_e^2) \cdot (v_f^2 + a_f^2) \cdot \chi^2$$

$$\text{and } C_2 = -4 \cdot Q_f \cdot a_e a_f \chi + 8 \cdot v_e v_f \cdot a_e a_f \cdot \chi^2$$

$Q_f$  is the electric charge of the final state fermion. The  $a_e, v_e, a_f, v_f$ , denote the vector and axial vector coupling constants of the  $Z_0$  to the electron and final state fermion currents respectively.  $\chi = g \cdot s \cdot M_Z^2 / (s - M_Z^2)$  and  $g = G_F / (\sqrt{2} \cdot \sin\theta_W)$  where  $G_F$  is the Fermi coupling constant and  $M_Z$  the mass of the  $Z_0$ . For  $e^+e^- \rightarrow e^+e^-$  the cross section is more complicated due to the presence of the t-channel.

The presence of the term  $C_2 \cdot \cos\theta$  in (1) leads to an angular asymmetry: which for  $\mu$  and  $\tau$  pairs ( $Q_f = -1$ ) is:

$$(2) \quad A = (F-B)/(F+B) = -1.5 \cdot a_e \cdot a_\mu \cdot \chi.$$

The small purely weak contribution  $\sim \chi^2$  was neglected; F and B denote the cross sections integrated over the forward and backward regions respectively. The asymmetry depends then only on the axial coupling constants of the  $Z_0$  to the leptons and via the propagator on the mass of the  $Z_0$ . Within the standard model the coupling constants are fixed by one free parameter, the electroweak angle  $\theta_W$  (see table 1). Using  $\sin^2\theta_W = 0.23$  from neutrino measurements<sup>3</sup> the predicted asymmetry is  $A = -0.094$  at  $s = 1182$  GeV<sup>2</sup>.

The total cross section is obtained by integrating (1):

$$(3) \quad \sigma_{fr}/\sigma_{QED} = C_1$$

Table 1: Weak Coupling Constants in the Standard Model

Particle	a	v	$v(\sin^2\theta=0.23)$
$e, \mu, \tau$	-1	$-1+4 \cdot \sin^2\theta$	-0.08
$u, c, (t)$	+1	$+1-8/3 \cdot \sin^2\theta$	0.39
$d, s, b$	-1	$-1+4/3 \cdot \sin^2\theta$	-0.69

where  $\sigma_{\text{QED}} = 4\pi\alpha^2/3s$  is the lowest order QED cross section. As the vector coupling constant of the electron, which is close to 0, appears in the interference term the expected deviations from QED are small.

Modifications of the expression 1-3 are expected from higher order contributions to the electroweak amplitude. Calculations to order  $\alpha^3$  are available for the pure QED cross sections<sup>9</sup>. They will be taken into account in the results quoted here. The corrections for the purely weak and electroweak interference term are partially available<sup>7</sup>. They are at Petra energies in general smaller than the corrections for the purely electromagnetic amplitudes and will not be corrected for. E.g. the muon asymmetry is changed from -9.4% to  $-(8.8 \pm 0.3)\%$  using calculations from ref. 7c.

### 3) LEPTONIC REACTIONS

#### 3.1) $e^+e^- \rightarrow e^+e^-$ and $\gamma\gamma$

For the analysis<sup>8</sup> of Bhabha scattering and the  $e^+e^-$  annihilation into a pair of photons an integrated luminosity of  $68.9 \text{ pb}^{-1}$  at an average cms energy of 34.6 GeV was used. The event selection was based on the barrel leadglass hodoscope and the tracking information was only used for charge separation and to distinguish Bhabha scattering from two photon production.

The principal cuts were:

- i) At least two energy clusters in the leadglass of energy  $E > E_{\text{beam}}/3$ .
  - ii) The acollinearity of the clusters had to be less than 100.
  - iii) Both tracks had to be within a fiducial region of  $|\cos\theta| < 0.76$ , where  $\theta$  is the angle between the track and the incoming positron.
- After the selection of events the remaining background came mainly from hadronic events,  $\tau$  pair production, and  $e^+e^- \rightarrow \gamma\gamma$ , where one of the electrons in the final state did not fulfill the cuts, but the

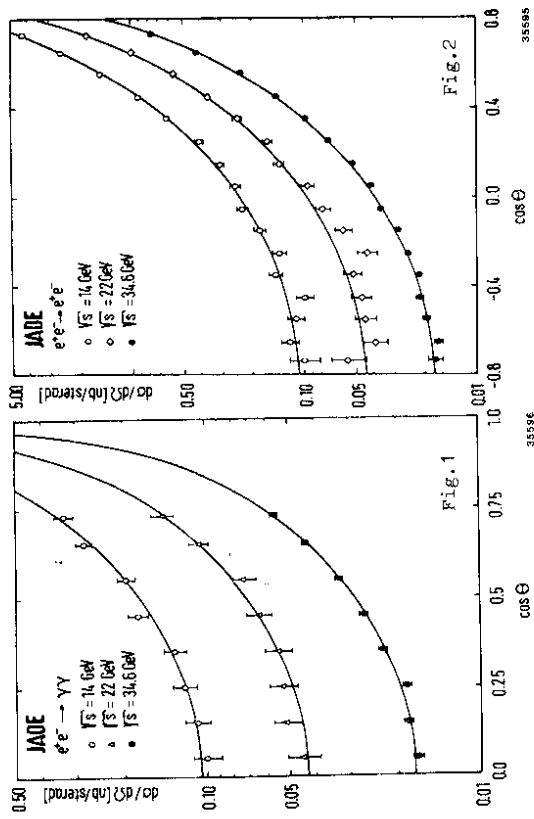


Fig. 1 and 2: The differential cross section for 1)  $e^+e^- \rightarrow \gamma\gamma$  and for 2)  $e^+e^- \rightarrow e^+e^-$  for three different cms energies. The curves are QED predictions.

photon nearby did. The background was reduced by scanning the events. The scan was also performed for simulated events and the rejected event fractions agreed well. The remaining background was subtracted statistically. Corrections were applied for small counter gaps, doubly converted  $e^+e^- \rightarrow \gamma\gamma$ , and charge misassignment. Radiative corrections up to order  $\alpha^3$  were applied<sup>9</sup>.

3.1.1)  $e^+e^- \rightarrow \gamma\gamma$ . In  $e^+e^- \rightarrow \gamma\gamma$  weak currents do not enter in lowest order. So the reaction is good for testing QED even at high energies.

In fig. 1 the differential cross section for the reaction  $e^+e^- \rightarrow \gamma\gamma$  is given as a function of  $\cos\theta$  for three different cms energies. The data points agree well with the prediction of lowest order QED (full lines). Cut off parameters  $\Lambda_c$  are traditionally used to parametrize limits on the deviations from QED.

$$(\frac{d\sigma}{d\Omega})_{\text{meas.}} / (\frac{d\sigma}{d\Omega})_{\text{QED}} = 1 \pm s^2/2\Lambda_c^4 \cdot (1 - \cos^2\theta)$$

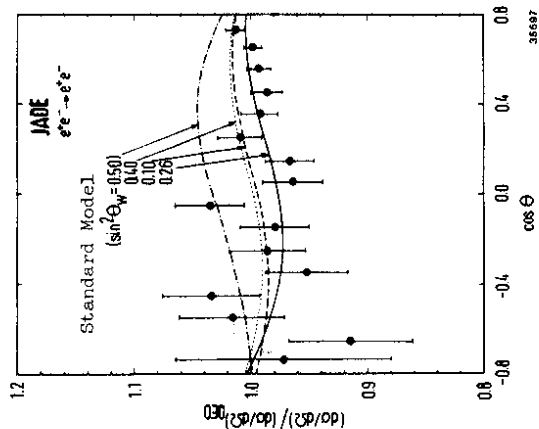


Fig.3: The ratio of the cross section for  $e^+e^- \rightarrow e^+e^-$  to the QED expectation compared to predictions of the standard model for different values of  $\sin^2\theta_W$ .

From the angular distribution at the highest cms energy 34.6 GeV, the following limits on the cut off parameters were derived:  $\Lambda_+ > 61$  GeV and  $\Lambda_- > 57$  GeV.  $\Lambda_+$  can be interpreted as the upper limit for  $M^2/\lambda$ , where  $M$  is the mass of a new heavy lepton and  $\lambda$  its coupling in units of the QED coupling constant  $e$ . The resulting upper limit is displayed in fig.8 (upper curve).

3.1.2)  $e^+e^- \rightarrow e^+e^-$ . In fig. 2 the differential cross section for Bhabha scattering is displayed as a function of  $\cos\theta$  for three cms energies. Agreement with QED to lowest order (full lines) is good. The comparison of data and QED can be done more conveniently by plotting the ratio of the two as a function of  $\cos\theta$  as in fig.3. The data points are compatible with 1 and therefore with QED. The effect of the electroweak interference term is displayed for different values of  $\sin^2\theta_W$ . The predicted deviations are small for  $\sin^2\theta_W = 0.23$ . The best fit to the data gives  $\sin^2\theta_W = 0.26 \pm 0.13$ .

3.2)  $e^+e^- \rightarrow \mu^+\mu^-, \tau^+\tau^-$

Data for  $e^+e^-$  annihilation into muon pairs come from 71.2 pb<sup>-1</sup> at an average cms energy of 34.4 GeV<sup>10</sup>; for  $\tau$  pairs only 30 pb<sup>-1</sup> were analysed. The  $\tau$  results will be updated soon. So no details will be given here.

The selection for  $\mu$  pair candidates starts by searching for pairs of tracks in a fiducial region of  $|\cos\theta| < 0.80$ , where  $\theta$  is the angle between track and positron beam direction. The following cuts are applied to reduce background from Bhabha scattering, two photon scattering, and  $\tau$  pair production:

- i) The tracks must come from the interaction region of the beams. They must be back to back, with an acollinearity less than 0.2 radians.
- ii) The energy deposited in the leadglass is compatible with that of a minimum ionizing particle. The particles must penetrate the muon filter.
- iii) The momenta are required to be  $p > E_{beam}/3$ .
- iv) A time-of-flight cut is made to remove cosmic ray muons.

Remaining background is removed by a scan of the events. In the final sample of 3200 muon pair candidates the background from cosmic ray muons and Bhabha scattering is negligible. Muon pairs from two photon scattering contribute 0.7% as calculated using ref.10.

$\tau$  pairs, where both taus decay leptonically into a muon are calculated to contribute 2% to the final event sample.

In fig.4a and b the angular distributions for muon pairs and  $\tau$  pairs are displayed. The data were corrected for QED contributions up to order  $\alpha^3$  using the programs by Berends and Kleiss<sup>9</sup>. For comparison the lowest order QED prediction (dashed line) and a fit of the parabola  $1 + \cos^2\theta + 8/3 \cdot A \cdot \cos\theta$  (solid line), as predicted by the electroweak interference effect are shown in the figures. The agreement of the data with the electroweak prediction is good.

The resulting values for the forward backward asymmetry are given in table 2, firstly as calculated directly from the number of events in the forward and backward directions for  $|\cos\theta| < 0.8$  (column 2). Secondly, the asymmetry from the fit mentioned above, which is extrapolated to  $\cos\theta = 1$ , is given in column 3 of table 1. The asymmetry expected in lowest order in the standard model using  $\sin^2\theta_W = 0.23$  ( $M_Z = 88.9$  GeV) is given in the last column of table 2.

The systematic error in the muon forward backward asymmetry of 1% in table 2 is mainly due to charge misassignment estimated by the number of like sign muon pairs and by performing combined fits of both tracks, if they were collinear within 10°. An error due to a possible twist of the apparatus was estimated by studying the

Table 2: Forward Backward Asymmetry for  $\mu\mu$  and  $\tau\tau$

Process	F-B/F+B	A from fit	A Stand.Mod.
$e^+e^- \rightarrow \mu^+\mu^-$	$-10.9 \pm 1.77$	$-11.63 \pm 1.88 \pm 1.0$	-9.4
$e^+e^- \rightarrow \tau^+\tau^-$	$-6.7 \pm 3.4$	$-7.9 \pm 4.0 \pm 2.9$	-9.2

neutrino data<sup>3</sup>, one obtains  $a_\mu = -1.14 \pm 0.26$ . This result confirms the assumption of electron muon universality of the standard model. If one would use the asymmetry including higher order corrections to the weak amplitude the coupling constant would be increased by only a third of the statistical error.

Assuming that the axial couplings are as predicted by the standard model, one can derive the mass of the weak neutral boson:  $M_Z = 61 \pm 9$  GeV. These limits correspond to 1 standard deviation. At the 95% confidence level  $M_Z > 50$  GeV.

3.3)  $e^+e^- \rightarrow e^+e^- \gamma, \gamma\gamma, \text{ and } \mu^+\mu^- \gamma$

Measurements of these processes are interesting for two reasons: They provide a test of the next-to-leading order calculations of the QED processes, which have to be used to correct all  $e^+e^-$  measurements. Secondly, the existence of an excited lepton,  $e^*$  or  $\mu^*$ , which decays into  $e\gamma$  or  $\mu\gamma$ , can be investigated in this channel.

3.3.1)  $e^+e^- \rightarrow e^+e^- \gamma$  and  $\gamma\gamma$ . A search was made for events containing at least three energy clusters in the leadglass. Two had to have an energy of  $E > E_{beam}/3$ , and one  $E > 0.1 \cdot E_{beam}$ . Background was suppressed by requiring  $\theta_{ik} > 10^\circ$  and  $E_{ik} > 3509$ , where  $\theta_{ik}$  were the respective angles between the clusters. 2513 (178) events were obtained for  $e^+e^- \gamma(\gamma\gamma)$  compared to 2388 (295) events expected by QED. Energy and angular distributions (figs. 5 and 6) show good agreement with the curves obtained using the calculations of ref. 9.

The invariant mass distribution of  $e\gamma$  is shown in fig. 7. No deviation from QED can be seen. The structures reflect energy and angular cuts. The 95% confidence level upper limit on the production of an  $e^*$  was calculated using the expression by Terazawa et al. 11. It is displayed in fig. 8,  $\lambda$  is the ratio between the new  $e^*$  coupling to the photon and that of the normal electron coupling.

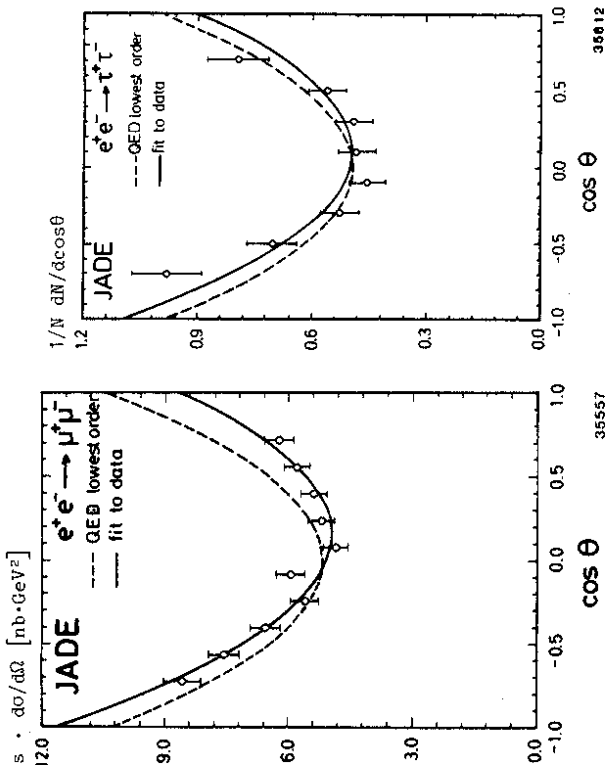


Fig. 4: Angular distributions for a)  $e^+e^- \rightarrow \mu^+\mu^-$  and b)  $e^+e^- \rightarrow \tau^+\tau^-$ , corrected for radiative effects to order  $\alpha^3$ . The full curves are parabola fits to the data, the dashed curves are QED predictions.

correlation of the momenta of the two tracks. The error due to remaining background is small as the only sizeable background comes from  $\tau$  decays, which have the same asymmetry as  $\mu$  pairs. Even if more cosmic rays, two photon or Bhabha events were present they would only reduce the absolute value of the measured asymmetry. The radiative corrections up to order  $\alpha^3$  show a positive forward backward asymmetry of +2% for the Jade cuts. This was corrected for in the data. Including the systematic error the measured muon asymmetry is 5 standard deviations from 0 and agrees well with the expectation from the standard model.

The measurement of the forward backward asymmetry can be interpreted within the standard model. The axial coupling constants were derived using expression 2 in chapter 2. With  $M_Z = 88.9$  GeV one gets:  $a_e \cdot a_\mu = 1.24 \pm 0.21$ . Using  $a_e = 1.09 \pm 0.11$  from the fit to all

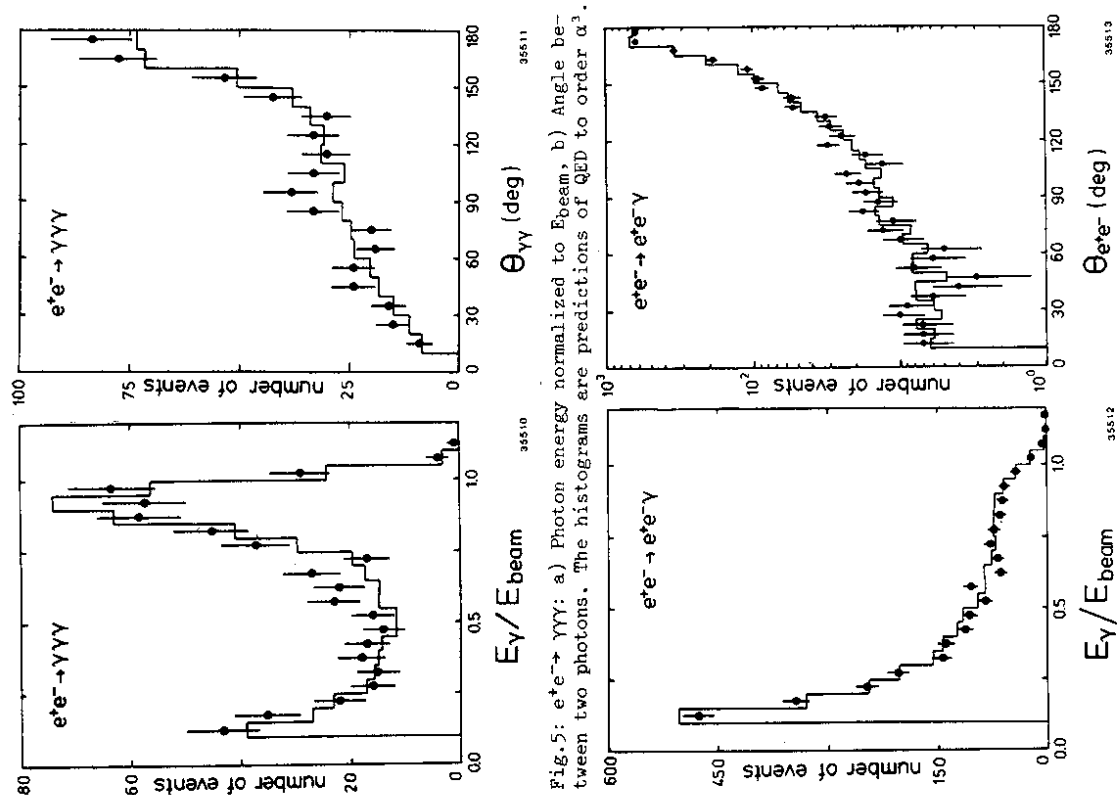


Fig. 5:  $e^+e^- \rightarrow \gamma\gamma\gamma$ : a) Photon energy normalized to  $E_{\text{beam}}$ , b) Angle between two photons. The histograms are predictions of QED to order  $\alpha^3$ .

Fig. 6:  $e^+e^- \rightarrow e^+e^-\gamma$ : a) Photon energy normalized to  $E_{\text{beam}}$ , b) Angle between  $e^+e^-$ . The histograms are predictions of QED to order  $\alpha^3$ .

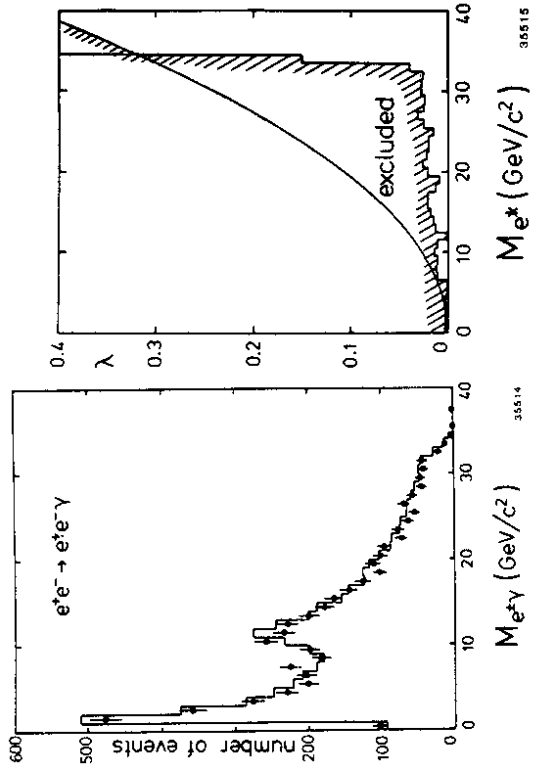


Fig. 7:  $e^+e^- \rightarrow e^+e^-\gamma$ : Invariant mass of the system electron-photon and positron-photon. The histograms are predictions of QED up to order  $\alpha^3$ .

Fig. 8: 95% confidence level upper limit for the production of an excited electron  $e^*$ . The smooth curve comes from  $e^+e^- \rightarrow \gamma\gamma$ , the histogram from  $e^+e^- \rightarrow e^+e^-\gamma$ .

3.3.2)  $e^+e^- \rightarrow \mu^+\mu^-\gamma$ . The selection for  $\mu^+\mu^-\gamma$  required in addition to the 2 charged tracks a photon of  $E > 1$  GeV, which had to be separated by at least 20c from the tracks. The sum of the momenta and the photon energy had to be larger than  $E_{\text{beam}}/3$ , the mass of the  $\mu$  pair larger than 1.2 GeV, and the sum of all three angles larger than 3550. 270 events were obtained compared with 298 predicted by QED.

The angular distribution is displayed in fig.9. It shows a strong forward backward asymmetry  $A = -0.39 \pm 0.08$ . This is due to the interference of the amplitudes for photon emission in the initial and final states. It is well described by the same calculations used for correcting the muon cross section. The asymmetries expected from QED alone and QED + weak effect are  $A_{\text{QED}} = -0.36 \pm 0.006$ ;  $A_{\text{QED+WEAK}} = -0.42 \pm 0.006$ , where the error is due to statistics of the Monte Carlo calculation.

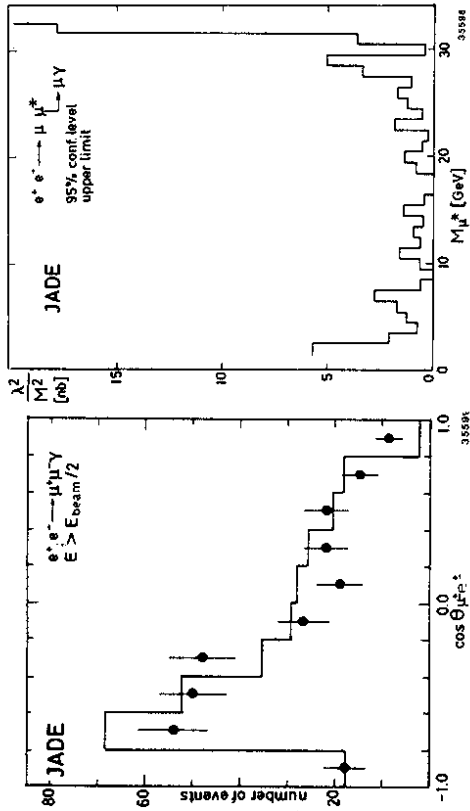


Fig.9:  $e^+e^- \rightarrow \mu^+\mu^-\gamma$ : Distribution of the angle between  $\mu^+e^+$  and  $\mu^-e^-$ . The histograms are predictions of QED up to order  $\alpha^3$ .

Fig.10: 95% conf. level upper limit on the production of an excited muon  $\mu^*$  from  $e^+e^- \rightarrow \mu^+\mu^-\gamma$ .

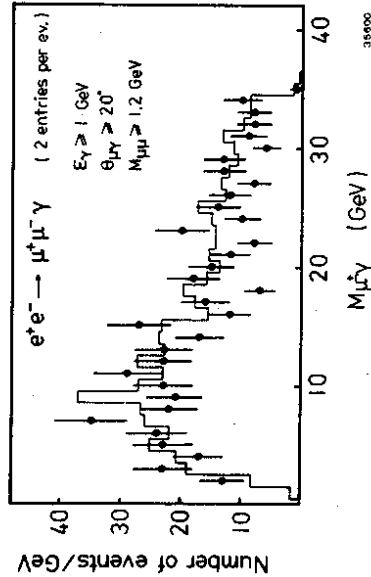


Fig.11:  $e^+e^- \rightarrow \mu^+\mu^-\gamma$  invariant mass of muon and photon. The histograms are predictions of QED to order  $\alpha^3$ .

The  $\mu\gamma$  invariant mass distribution is shown in fig.11. There is no structure showing a deviation from QED. The 95% conf. level upper limit for the production of an excited muon is again obtained using the Terazawa et al.<sup>11</sup> expressions. It is given in fig.10.

4)  $e^+e^- \rightarrow q\bar{q} \rightarrow$  HADRONS

In the Quark Parton Model (QPM) the total cross section ratio  $R$  is given by:

$$R = \sigma(e^+e^- \rightarrow q\bar{q}) / \sigma_{\text{QED}} = 3 \cdot \sum Q_f^2$$

where  $\sigma_{\text{QED}}$  is the lowest order QED cross section for muon pairs and the sum runs over all available flavours. The factor 3 takes into account the three colours of quarks. For 5 quarks the QPM prediction is  $R = 11/3$ . QCD<sup>12</sup> predicts a correction factor  $1 + \alpha_s/\pi$  for this ratio due to gluon emission, where  $\alpha_s$  is the running coupling constant. With  $\alpha_s = 0.18$  this correction amounts to a change in  $R$  of approximately 5%, almost energy independent in the Petra range of energies. The higher order QCD corrections are negligible.

Another modification of the simple QPM formula is due to the electroweak interference, which within the framework of the standard model, using  $\sin^2\theta_W = 0.23$ , leads to an energy dependent modification of  $\sim 0.3\%$  at  $W = 14$  GeV, and  $\sim 1\%$  at  $W = 34$  GeV. Values of  $\sin^2\theta_W$  that differ appreciably from 0.23 lead to a stronger energy dependence as shown in fig.13.

In order to study these effects Jade has carefully investigated the contributions of systematic error to  $R$  and tried to reduce them. The total cross section at each energy point is calculated using the following quantities:

$$R = (N_{\text{MH}} - N_{\text{BG}}) / (L \cdot \epsilon \cdot (1 + \delta)) / \sigma_{\mu\mu}$$

where  $N_{\text{MH}}$  is the number of multihadronic events,  $N_{\text{BG}}$  the number of remaining background events,  $L$  the luminosity,  $\delta$  the radiative corrections, and  $\epsilon$  the acceptance. In the following the determination of each of these quantities and their errors is briefly described. The number of multihadronic events  $N_{\text{MH}}$  was obtained using the following selection criteria:

- 1) A minimum amount of shower energy in the barrel part of the leadglass was required depending on the cms energy; at  $W > 24$  GeV the requirement was 3 GeV.
- 2) At least 4 tracks should have come from the interaction region, 3 must have  $P_t > 0.5$  GeV. The 1 topology - namely 1 track opposite to 3 - was rejected.
- 3)  $E_{\text{vis}} > E_{\text{beam}}$ , where  $E_{\text{vis}}$  was the sum of neutral and charged energy.



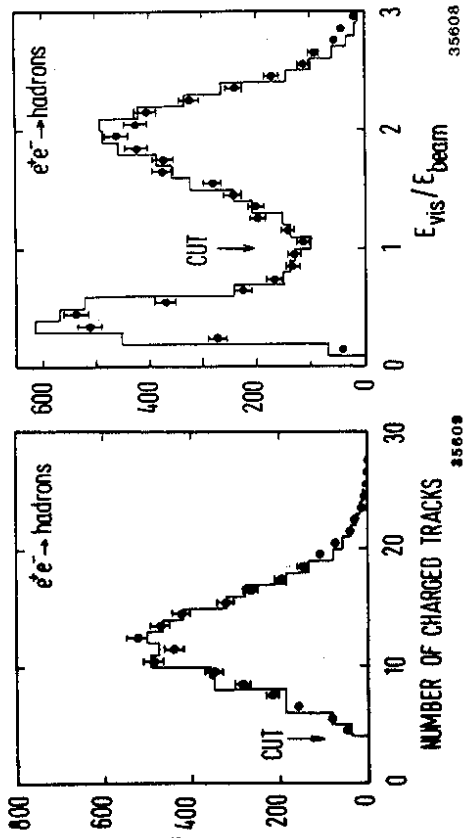


Fig. 12: a) Multiplicity distribution. b)  $E_{vis}/E_{beam}$  distribution for  $|p_{bal}| < 0.4$ . The histograms are Monte Carlo predictions.

4)  $|p_{bal}| \leq 0.4$ ; where  $p_{bal} = E_{p1z}/E_{vis}$  is the longitudinal energy balance,  $p1z$  is the projection of the momenta on the beam direction.  
 5) the event vertex was required to be within 150 mm from the interaction point in the beam direction.  
 Two examples of distribution are shown in fig. 12.

All events were scanned. The main background came from hadron production via two photon exchange characterized by low visible energy (fig. 12b) and  $\tau$  pair production. Both contributions were calculated by Monte Carlo programs. The systematic error on the 2 photon background was estimated by varying the cut in the visible energy. Furthermore the amount of 2 photon background could be greatly reduced by cutting out events in the forward region of the detector. Within statistics no change in R was observed. The systematic error of the  $\tau$  background was obtained by a variation of the decay branching ratios. The background from beam gas events, Bhabha scattering, two photon production, and cosmic rays were reduced to a negligible fraction after scanning.

The acceptance was calculated using the Lund Monte Carlo program<sup>13</sup>, which best reproduces the experimental distributions including the multiplicity (fig. 12a).

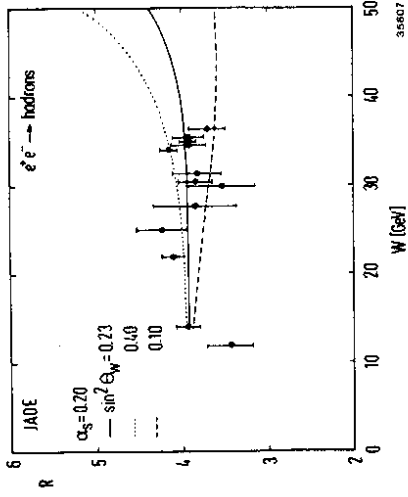


Fig. 13:  $e^+e^- \rightarrow$  hadrons. The total cross section normalized to  $\sigma_{\mu\mu}$  as a function of cms energy. The error bars include statistical and point-to-point systematic errors. The curves show theoretical calculations including QCD and electroweak corrections for  $\alpha_s = 0.20$  and different values of  $\sin^2\theta_W$ .

Radiative corrections were calculated using the programs of Berends and Kleiss<sup>9</sup>. Mainly the uncertainty in the vacuum polarization term due to the uncertainty in the total hadronic cross section leads to the systematic errors in table 3. The error due to the radiative corrections of orders higher than  $\alpha^3$  was not taken into account.

The luminosity was calculated using Bhabha events in the barrel part of the detector ( $|\cos\theta| < 0.76$ ). Uncertainties in the acceptance and radiative corrections are given as a normalization error, while errors due to small counter gaps, calibration uncertainties, and background subtraction are included in the point to point error.

The systematic errors from the various contributions are summarized in table 3 for two values of the cms energy. For  $W = 35$  GeV they add up to 3%. The total hadronic cross section ratio is shown in fig. 13 as a function of cms energy. In the error bars the statistical as well as the point to point systematic error are included. The points are compatible with being constant and  $\langle R \rangle = 3.97 \pm 0.05$  (stat)  $\pm 0.10$  (sys). This value is  $8.3\% \pm 3.0\%$  above prediction of the QPM for 5 quarks including colour.

A fit of the data points for  $W > 14$  GeV to the cross section was performed including electroweak and QCD corrections<sup>14</sup> with  $\alpha_s$

Table 3: Systematic Error of R in %.

Source	$W \leq 14$ GeV	22-37 GeV
Background	1.6	1.6
Rad. Corrections	1.1	0.8
Det. Efficiency	2.5	1.5
Lumi point-to-point	1.0	1.0
Lumi normalisation	1.5	1.5
TOTAL	3.6	3.0
Point-to-point Normalisation	2.7	1.9
	2.4	2.4

and  $\sin^2\theta_W$  as free parameters. In addition to the data points the absolute normalisation with the overall systematic error was used as a measured point in calculating  $\chi^2$ . The result is  $\alpha_s = 0.20 \pm 0.08$  and  $\sin^2\theta_W = 0.23 \pm 0.05$ , where the errors include statistical as well as systematic errors. The correlation of errors is small. The best fit is shown in fig.13 as a full curve. The minimum  $\chi^2$  is 9.8 for 10 degrees of freedom. A second minimum at  $\sin^2\theta_W = 0.54$  is excluded by the lepton data of the Jade experiment.

5) SEARCH FOR NEW HEAVY LEPTONS

The Jade collaboration has performed searches<sup>15</sup> for a sequential lepton beyond the  $\tau$ , which will be produced in  $e^+e^- \rightarrow L^+L^-$ , and at the same time for a neutral electronlike lepton produced by  $W$  exchange  $e^+e^- \rightarrow E^0V_e$  or  $E^0V_e$ . Both V-A and V+A couplings of the  $E^0$  to the  $W$  were assumed, leading to slightly different limits<sup>16</sup>.

The decay of these new leptons then proceeds in the standard way:  $L^{\pm} \rightarrow V_l W^{\pm}$  and  $E^0 \rightarrow e^+W^-$ . The  $W$  decays to leptons or quarks. The branching fractions depend on the mass of the heavy lepton below  $\sim 14$  GeV, above that they are constant,  $\sim 35\%$  to (ud) and (cs) pairs, and  $\sim 10\%$  to each pair of leptons<sup>17</sup>.

A luminosity of  $37 \text{ pb}^{-1}$  at an average cms energy of 34.2 GeV was used. The upper limits were obtained by applying a certain set of cuts to the data and to simulated events and comparing the expected numbers to the real events.

Depending on the mass range of the lepton different event topologies were used. For L and  $E^0$  of high masses acoplanar two jet

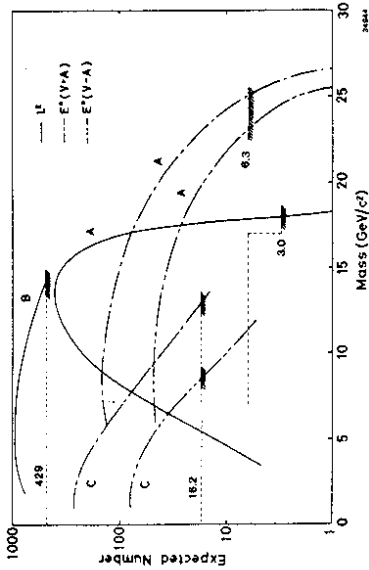


Fig.14: 95% confidence level upper limits for the production of a new heavy sequential lepton L and a new heavy electronlike lepton  $E^0$ . For an explanation of the curves see text.

events were searched for. The 95% confidence upper limits as a function of mass are given in fig.14 in the curves labelled A. A heavy lepton L of lower mass was searched for in events containing a jet opposite to an isolated track. The limit is displayed in curve B of fig.14. Finally for the low mass  $E^0$  a single jet opposite to an empty cone was searched for. The upper limits are given by curves C in fig.14.

In conclusion: A new heavy sequential lepton is excluded up to a mass of 18 GeV. A neutral heavy lepton with V+A coupling is excluded below 24.5 GeV and excluded below 22.5 GeV with V-A coupling.

SUMMARY OF RESULTS:

- 1) The Jade collaboration has performed tests of QED and electroweak interactions using the processes:  $e^+e^- \rightarrow e^+e^-$ ,  $\gamma\gamma$ ,  $\mu^+\mu^-$ ,  $\tau^+\tau^-$ ,  $e^+e^- \gamma$ ,  $\gamma\gamma$ ,  $\mu^+\mu^-$ . For  $\mu^+\mu^-$  a forward backward asymmetry of  $- (11.76 \pm 1.88 \pm 1.0)\%$  was observed which agrees with the prediction of the standard model using  $\sin^2\theta_W = 0.23$ . The limit on the mass of the weak neutral boson is  $M_Z > 50$  GeV at 95% confidence level. All other reactions agree with QED including terms up to  $\alpha^3$ .
- 2) The systematic error in  $e^+e^- \rightarrow$  hadrons was reduced to 3% at high energy. The measured cross section was used to determine  $\alpha_s = 0.20 \pm 0.08$  and  $\sin^2\theta_W = 0.23 \pm 0.05$  simultaneously. The errors include statistical as well as systematic errors.
- 3) Excited electrons or muons decaying into lepton and  $\gamma$  could be excluded for masses up to  $\sim 32$  GeV.
- 4) A new heavy sequential lepton was excluded below 18 GeV, a new neutral electronlike heavy lepton below  $\sim 24.5$  GeV if it has V + A coupling, below 22.5 GeV for V - A coupling. All limits are at 95% confidence level.

REFERENCES

- 1) The Jade Collaboration has members from the following institutions: DESY, Universities of Hamburg, Heidelberg, Lancaster, Manchester, Rutherford Appleton Laboratory, University of Tokyo.
- 2) S.L. Glashow, Nucl. Phys. 22 (1961) 579; Rev. Mod. Phys. 52 (1980) 539 (1980) 539
- A. Salam, Phys. Rev. 127 (1962) 331; Rev. Mod. Phys. 52 (1980) 525; S. Weinberg, Phys. Rev. Lett. 19 (1967) 1264; Rev. Mod. Phys. 52 (1980) 514.
- 3) J.E. Kim et al., Rev. Mod. Phys. Vol. 53 (1981) 211; F.W. Buesser, Invited Talk at the DESY Workshop on Electroweak Interactions, DESY T-82-05 (1982); F.W. Krenz, Compilation on Neutrino Electron Scattering Data and Remarks on Lepton Coupling Constants, FITHA 82/26.
- 4) C. Prescott et al., Phys. Lett. 77B (1978) 347; C. Prescott et al., Phys. Lett. 84B (1979) 524.
- 5) Jade Collaboration, W. Bartel et al., Phys. Lett. 88B (1979) 171
- H. Drumm et al., Wire Chamber Conference 1980, Ed.W. Bartel and M. Regler, North Holi. Publ. Comp., Page 333.
- 6) R. Budny, Phys. Lett. 55B (1975) 227;
- 7) G. Passarino and M. Veltman, Nucl. Phys. B160 (1979) 151; M. Greco et al., Nucl. Phys. B160 (1979) 208
- F.A. Berends, R. Kleiss, and S. Jadach: Nucl. Phys. B202 (1982) 63; E.A. Paschos, Private Communication;
- W. Metzler, Private Communication.
- 8) Jade Collaboration; W. Bartel et al., Phys. Lett. 92B (1980) 206; Jade Collaboration, W. Bartel et al., to be published.
- 9) F.A. Berends et al., Nucl. Phys. B57 (1973) 381; Nucl. Phys. B61 (1973) 414; Nucl. Phys. B63 (1973) 381; Nucl. Phys. B63 (1973) 452; Nucl. Phys. B68 (1973) 541; Nucl. Phys. B177 (1981) 237; Nucl. Phys. B178 (1981) 141; F.A. Berends, and R. Kleiss, DESY-Report 80-66 (1980).
- 10) Jade Collaboration, W. Bartel et al., Phys. Lett. 108B (1982) 140.
- 11) Terazawa et al., Ins.-Rep.-443, Dec. 1981, University of Tokyo.
- 12) M. Dine et al., Phys. Rev. Lett. 43 (1979) 668; K.G. Chetyrkin et al., Phys. Lett. 85B (1979) 277; W. Celmaster et al., Phys. Rev. Lett. 44 (1979) 44
- 13) B. Andersson et al., Phys. Lett. 94B (1980) 211
- 14) J. Jersak et al., Phys. Lett. 98B (1981) 363
- 15) Jade Collaboration, W. Bartel et al., Phys. Lett. 123B (1983) 353
- 16) J.D. Bjorken et al., Phys. Rev. D7 (1973) 887; F. Bletzacker et al., Phys. Rev. D16 (1977) 2115; K. Fujikawa, Phys. Rev. D17 (1978) 1841; M. Gourdin et al., Nucl. Phys. B164 (1980) 387
- 17) Y.S. Tsai, Phys. Rev. D4 (1971) 2821; Slac-Pub-2450 (1979)
- 18) J.A.M. Vermaseren, Proc. of the Intern. Workshop on Y Y Collisions, Amiens 1980, published by Springer Verlag; Lecture Notes in Physics 134 (1980) 269

